

Synthesis and Characterization of V-SBA-1 Cubic Mesoporous Molecular Sieves

Lian-Xin Dai,^{*,†} Kenji Tabata,^{†,‡} Eiji Suzuki,^{†,‡} and Takashi Tatsumi[§]

Research Institute of Innovative Technology for the Earth (RITE), 9-2 Kizugawadai, Kizu-cho, Soraku-gun, Kyoto 619-0292, Japan, Graduate School of Materials Science, Nara Institute of Science and Technology (NAIST), 8916-5 Takayama, Ikoma, Nara 630-0101, Japan, and Division of Materials Science and Chemical Engineering, Faculty of Engineering, Yokohama National University, 79-5 Tokiwadai, Hodogaya-ku, Yokohama 240-8501, Japan

Received July 17, 2000. Revised Manuscript Received October 31, 2000

Vanadosilicate V-SBA-1, which incorporated more than 4 wt % vanadium ($\text{Si}/\text{V} < 20$) in cubic mesoporous molecular sieves, was directly synthesized under strongly acidic conditions and characterized by various techniques. Powder X-ray diffraction (XRD) showed that the resultant samples had a well-ordered cubic SBA-1 structure. The structural regularity of V-SBA-1 was improved by preparation under highly acidic conditions. N_2 adsorption/desorption measurements confirmed that an additional large mesopore (≈ 40 Å) was simultaneously produced with the main one (≈ 20 Å) in SBA-1 after the incorporation of vanadium into the SBA-1 framework. UV-vis and laser Raman results revealed that the incorporated vanadium species existed in a highly dispersed state and had tetrahedral coordination.

Introduction

Vanadosilicate is known to be an excellent hydrocarbon oxidation catalyst by use of hydrogen peroxide as an oxidant.^{1–4} In the case of liquid-phase reaction, however, large organic molecules are sterically prevented from diffusing into zeolite pores and this limits the usefulness of these catalysts for the oxidation of large organic compounds. Recently, a new family of mesoporous molecular sieves, designated as M41S, was discovered by Mobil scientists.^{5,6} These materials have uniform pore sizes larger than 20 Å and large surface areas ($> 1000 \text{ m}^2 \text{ g}^{-1}$). The incorporation of vanadium into the mesoporous molecular sieves is of considerable interest for catalytic applications. So far, however, most studies have dealt with the one-dimensional and hexagonal form MCM-41,^{7–9} MCM-48, the cubic member

of the M41S family, has been investigated only in a limited number of studies.¹⁰ Very recently, Huo et al. reported the synthesis of a novel mesoporous molecular sieve with three-dimensional channel systems denoted SBA-1 under strongly acidic synthesis conditions.^{11–14} It has been found that Al, Sn, and Zn metal elements can be grafted onto siliceous frameworks of SBA-1 by using the metal-implantation method.¹⁵ Vanadium-incorporating three-dimensional mesoporous SBA-1 has been attracting much attention because of its highly feasible catalytic property for the oxidation of large organic compounds. Morey et al.¹⁶ investigated the incorporation of V into the SBA-1 phase using VCl_4 (aq) as the metal atom source. They reported that a hexagonal phase (SBA-3) was observed in the region of Si/V less than 18 in the initial mixture, although a cubic phase (SBA-1) was formed in the region of Si/V larger than 18.

In the current research, we have aimed at preparing vanadosilicate V-SBA-1 mesoporous molecular sieves with a direct synthesis method. A systematic investigation of V-SBA-1 materials by powder X-ray diffraction (XRD), nitrogen adsorption/desorption, inductively

* To whom correspondence should be addressed. E-mail: dai@rite.or.jp. Phone: +81-774-75-2305. Fax: +81-774-75-2318.

[†] RITE.

[‡] NAIST.

[§] Yokohama National University.

(1) Miyamoto, A.; Medhanavny, D.; Inui, T. *Appl. Catal.* **1986**, *28*, 89.

(2) Rigutto, M. S.; Van Bekkum, H. *Appl. Catal.* **1991**, *68*, L1.

(3) Prasad Rao, P. R. H.; Kumar, R.; Ramaswamy, A. V.; Ratnasamy, P. *Zeolites* **1993**, *13*, 663.

(4) Reddy, K. R.; Ramaswamy, A. V.; Ratnasamy, P. *J. Catal.* **1993**, *143*, 275.

(5) Kresge, C. T.; Leonowicz, M. E.; Roth, W. J.; Vartuli, J. C.; Beck, J. S. *Nature* **1992**, *359*, 710.

(6) Beck, J. S.; Vartuli, J. C.; Roth, W. J.; Leonowicz, M. E.; Kresge, C. T.; Schmitt, K. D.; Chu, C. T.-W.; Olson, D. H.; Sheppard, E. W.; McCullen, S. B.; Higgins, J. B.; Schlenker, J. L. *J. Am. Chem. Soc.* **1992**, *114*, 10834.

(7) Zhang, W.; Wang, J.; Tanev, P. T.; Pinnavaia, T. J. *J. Chem. Soc., Chem. Commun.* **1996**, 979.

(8) Luan, Z.; Xu, J.; He, H.; Klinowski, J.; Kevan, L. *J. Phys. Chem.* **1996**, *100*, 19595.

(9) Wei, D.; Wang, H.; Feng, X.; Chueh, W. T.; Ravikovitch, P.; Lyubovskiy, M.; Li, C.; Takeguchi, T.; Haller, G. L. *J. Phys. Chem. B* **1999**, *103*, 2113.

(10) Schumacher, K.; Grun, M.; Unger, K. K. *Microporous Mesoporous Mater.* **1999**, *27*, 201.

(11) Huo, Q.; Margolese, D. I.; Ciesla, U.; Demuth, D. G.; Feng, P.; Gier, T. E.; Sieger, P.; Firouzi, A.; Chmelka, B. F.; Schuth, F.; Stucky, G. D. *Chem. Mater.* **1994**, *6*, 1176.

(12) Huo, Q.; Margolese, D. I.; Stucky, G. D. *Chem. Mater.* **1996**, *8*, 1147.

(13) Huo, Q.; Margolese, D. I.; Ciesla, U.; Feng, P.; Gier, T. E.; Sieger, P.; Leon, R.; Petroff, P. M.; Schuth, F.; Stucky, G. D. *Nature* **1994**, *368*, 317.

(14) Huo, Q.; Leon, R.; Petroff, P. M.; Stucky, G. D. *Science* **1995**, *268*, 1324.

(15) Ryoo, R.; Jun, S.; Kim, J. M.; Kim, M. J. *J. Chem. Soc., Chem. Commun.* **1997**, 2225.

(16) Morey, M. S.; Davidson, A.; Stucky, G. D. *J. Porous Mater.* **1998**, *5*, 195.

coupled plasma emission spectroscopy (ICP), diffuse reflectance UV–visible (UV–vis), and laser Raman spectroscopy are carried out for their characterizations. The results will show that a considerably large amount of V can be incorporated into the framework of SBA-1 and the vanadium species is present in a highly dispersed state and has tetrahedral coordination.

Experimental Section

Surfactant Preparation. The surfactant cetyltriethylammonium bromide [$C_{16}H_{33}(C_2H_5)_3NBr$, CTEABr] was synthesized by the reaction of cetyl bromide with an equimolar amount of triethylamine in acetone solution under reflux conditions for 7 days. The resulting CTEABr was purified three times by recrystallizing from acetone solution.

Synthesis of Mesoporous Materials. Cubic vanadosilicate mesoporous molecular sieves, V-SBA-1, were synthesized under acidic conditions using CTEABr as a surfactant, tetraethyl orthosilicate [$Si(OC_2H_5)_4$, TEOS] as a silica source, and ammonium vanadium (NH_4VO_3) as a vanadium source in an aqueous solution of hydrochloric acid.

A typical synthesis was conducted as follows: CTEABr, HCl (35%), and distilled water were mixed to obtain a homogeneous solution, which was cooled at 273 K and stirred for 30 min. TEOS (precooled to 273 K) and vanadium precursor solution (0.25 mol $V L^{-1}$) were added to the above mixture with vigorous stirring. After being stirred for 5 min, the mixture was allowed to react at 273 K under static conditions for 6 h. The molar composition of the gel was as follows: TEOS/CTEABr/HCl/ H_2O/V 1/0.13/(5–20)/(125–250)/0.2. The precipitate was filtered after 6 h, dried (without washing) at 393 K overnight, and then calcined in air at 903 K for 4 h. Pure siliceous SBA-1 was synthesized with the same procedure (HCl/TEOS = 10 and $H_2O/TEOS = 125$) in the absence of vanadium.

Characterization. Produced mesoporous materials were examined by XRD (RIGAKU, RINT-2000) with Cu K α radiation at 20 kV and 50 mA. XRD patterns were obtained in the region from 1.5° to 10° with a scan speed of 1° min^{-1} .

Nitrogen adsorption/desorption isotherms were measured at the liquid nitrogen temperature (YUASA-IONICS, AUTOSORB-1C). Calcined samples were outgassed at 473 K for at least 5 h before measurements. Surface areas were calculated by using the BET method. Pore volumes were estimated at a relative pressure of $p/p_0 > 0.99$, assuming full surface saturation of nitrogen. Pore size distributions were obtained from the N_2 desorption branch by using the Dolimore–Heal model.

Vanadium contents in the calcined V-SBA-1 samples were determined by ICP (SEIKO, SPS-1200VR) after solubilization of the samples in HF/HCl solutions.

Diffuse reflectance UV–vis spectra were measured with a HITACHI U-3500 spectrophotometer equipped with a reflectance attachment and Al_2O_3 was used as reference. Powder samples were loaded in a quartz cell, and spectra were collected in the range of 200–600 nm.

Laser Raman spectra were obtained with a RENISHAW SYSTEM-1000 spectrometer at room temperature. The samples were excited by an He–Ne ion laser at 632.8 nm at a power of 17 mW (0.17 mW for V_2O_5) and an exposed time of 60 s (10 s for V_2O_5). The spectral resolution is estimated to be 1 cm^{-1} .

Results and Discussion

The powder X-ray diffraction patterns of the as-synthesized and calcined siliceous SBA-1 and various V-SBA-1 products are presented in Figures 1 and 2, respectively. Table 1 gives the preparation conditions and the textural properties of resulting mesoporous molecular sieves. As displayed in Figures 1 and 2, all the as-synthesized and calcined samples showed the typical characteristic patterns of the cubic phase of SBA-

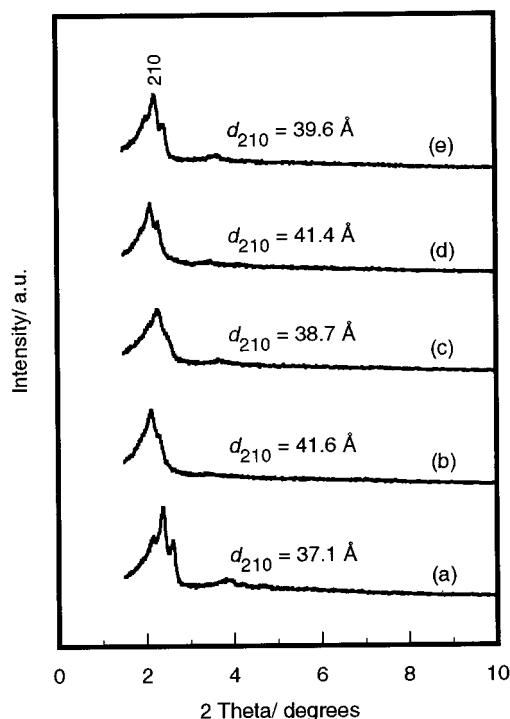


Figure 1. XRD patterns for the various as-synthesized samples: (a) siliceous SBA-1; (b) V-SBA-1(A); (c) V-SBA-1(B); (d) V-SBA-1(C); (e) V-SBA-1(D).

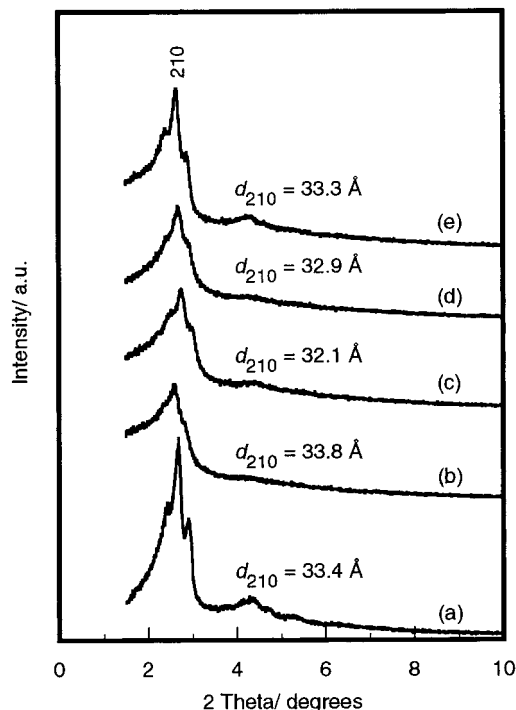


Figure 2. XRD patterns for the various calcined samples: (a) siliceous SBA-1; (b) V-SBA-1(A); (c) V-SBA-1(B); (d) V-SBA-1(C); (e) V-SBA-1(D).

1, which can be indexed to the $Pm\bar{3}n$ space group, matching well with that reported in the literature.^{11,12} However, the structure of V-SBA-1 was less ordered than that of pure silica SBA-1. The increase in the d_{210} spacing of as-synthesized V-SBA-1 samples compared to that of its pure silica analogue (Figure 1) confirms the presence of vanadium in the silicate framework. This is consistent with what would be expected because

Table 1. Synthesis Conditions and Physical Properties of Various Calcined Samples

sample	V (wt %)	Si/V ratio	S_{BET} ($\text{m}^2 \text{g}^{-1}$)	pore volume ($\text{cm}^3 \text{g}^{-1}$)	average pore diameter (\AA)
V-SBA-1(A) ^a	5.5	14	1257	0.70	22.3
V-SBA-1(B) ^b	5.1	15	1218	0.66	21.6
V-SBA-1(C) ^c	5.0	16	1412	0.74	21.0
V-SBA-1(D) ^d	4.0	20	1365	0.71	20.7
SBA-1 ^e	0.0		1494	0.87	23.2

^a 1/0.13/5/125/0.2 TEOS/CTEABr/HCl/H₂O/V. ^b 1/0.13/10/125/0.2 TEOS/CTEABr/HCl/H₂O/V. ^c 1/0.13/10/250/0.2 TEOS/CTEABr/HCl/H₂O/V. ^d 1/0.13/20/250/0.2 TEOS/CTEABr/HCl/H₂O/V. ^e 1/0.13/10/125 TEOS/CTEABr/HCl/H₂O.

the V–O bond length is longer than that of Si–O.¹⁷ However, there is no evident difference in the d_{210} spacing between calcined V-SBA-1 and a siliceous one (Figure 2).

The structural regularity of the cubic phase could be controlled by varying the HCl content in the gel. An increase in the amount of HCl in the starting gel (samples A and B: HCl/TEOS = 5 → 10; samples C and D: HCl/TEOS = 10 → 20) enhanced the order of cubic structures. This result is consistent with the observation by Kim and Ryoo,¹⁸ who reported that higher acidic conditions were favorable for the formation of cubic siliceous SBA-1. This can be explained by the surfactant-silica assembly mechanism ($\text{S}^+\text{X}^-\text{I}^+$) proposed by Huo and co-workers.^{11,12} Furthermore, when twice the amount of HCl and H₂O was added to the gel (with the other composition fixed), much more ordered V-SBA-1 materials (C and D samples compared to A and B ones, respectively) were obtained.

As shown in Figures 1 and 2 and Table 1, the direct synthesis of V-SBA-1 by using NH_4VO_3 as a precursor gave a fairly well-ordered cubic structure with more than 4 wt % V (Si/V < 20) in contrast to the hexagonal structure reported by Morey et al.¹⁶ Therefore, the anionic VO_3^- species seem to be favorable for the incorporation of V into the SBA-1 framework according to the $\text{S}^+\text{X}^-\text{I}^+$ synthesis route.^{11,12} A slight decrease in the amount of incorporated vanadium formed at higher acidic conditions in Table 1 (samples B and D compared to A and C, respectively) should be attributed to higher solubility of the V species in the concentrated aqueous solution of HCl.

Figures 3 and 4 show the N₂ adsorption/desorption isotherms and their corresponding pore size distribution curves obtained from the desorption branch for the calcined siliceous SBA-1 and various V-SBA-1 samples. For V-SBA-1 samples, the isotherms and pore size distribution curves were quite similar. However, they were different from those for siliceous SBA-1. Besides the sharp inflection at a relative pressure of $p/p_0 = 0.1-0.3$ corresponding to capillary condensation within the uniform mesopores, an obvious hysteresis loop at $p/p_0 > 0.5$ (Figure 3b–e), which indicated that the larger pores were filled at higher relative pressures, was also detected. The siliceous SBA-1 showed a very narrow pore size distribution with a pore diameter of $\approx 20 \text{ \AA}$ (Figure 4a). This indicated the structural uniformity of siliceous SBA-1 material. For the V-incorporated samples,

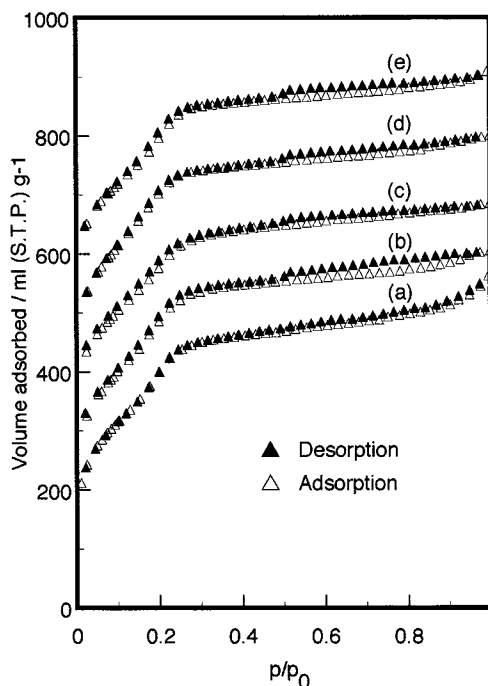


Figure 3. Nitrogen adsorption/desorption isotherms for the various calcined samples: (a) siliceous SBA-1; (b) V-SBA-1(A); (c) V-SBA-1(B); (d) V-SBA-1(C); (e) V-SBA-1(D).

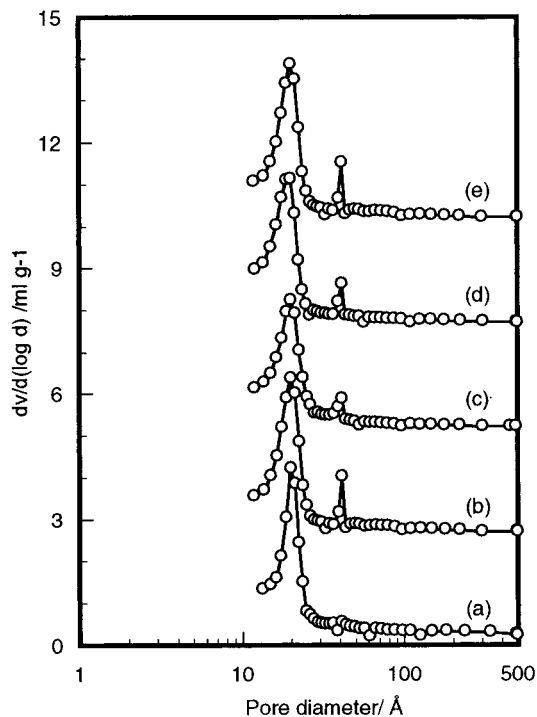


Figure 4. Pore size distribution for the various calcined samples: (a) siliceous SBA-1; (b) V-SBA-1(A); (c) V-SBA-1(B); (d) V-SBA-1(C); (e) V-SBA-1(D).

not only the same main pore size distribution ($\approx 20 \text{ \AA}$) (Figure 4b–e) but also additional larger mesopores with a pore diameter of around 40 \AA were observed. Because this newly appeared larger pore was not detected for the siliceous one, it was assumed that this pore was accompanied by the incorporation of V into the SBA-1 framework.

The presence of a cubic phase of SBA-1 has been suggested to have an ordered three-dimensional struc-

(17) Reddy, K. M.; Moudrakovski, I.; Sayari, A. *J. Chem. Soc., Chem. Commun.* **1994**, 1059.

(18) Kim, M. J.; Ryoo, R. *Chem. Mater.* **1999**, *11*, 487.

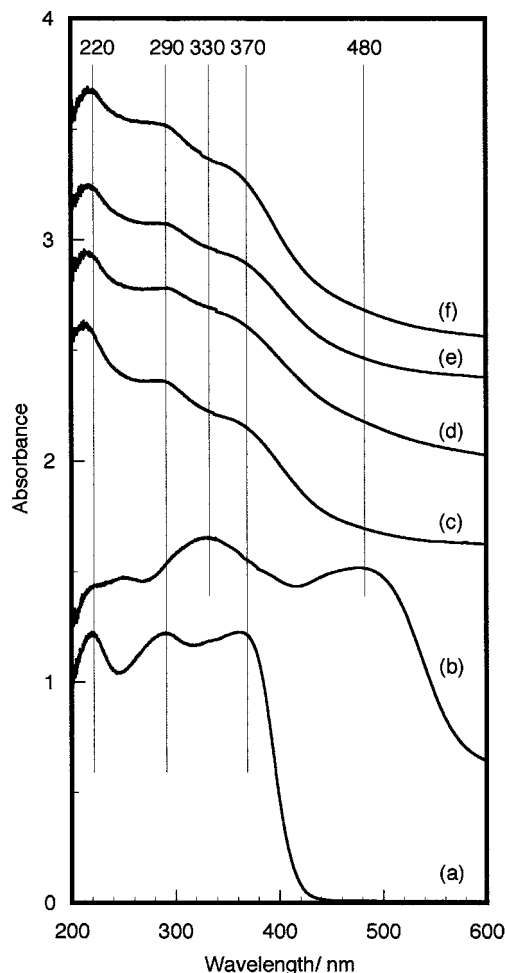


Figure 5. Diffuse reflectance UV-vis spectra of the various as-synthesized samples and reference compounds: (a) NH_4VO_3 ; (b) V_2O_5 ; (c) V-SBA-1(A); (d) V-SBA-1(B); (e) V-SBA-1(C); (f) V-SBA-1(D).

ture with two types of globular cages,¹³ forming a continuous porous network.¹⁴ Recently, Kruk et al. found that the BJH mesopore size distribution for siliceous SBA-1 was broad and featured a noticeable shoulder at about 26 Å, which might arise from the presence of smaller mesoporous cages in addition to larger ones (≈ 35 Å).¹⁹ It should be noted that the V-SBA-1 materials synthesized in the present study had remarkably narrow pore size distributions with main mesopores and secondary ones.

As given in Table 1, both the siliceous and V-incorporated SBA-1 mesoporous materials exhibited considerably high BET specific surface areas more than $1000 \text{ m}^2 \text{ g}^{-1}$. A slight decrease in the mesopore surface areas and pore volumes due to the incorporation of vanadium could be explained by some destruction of the pore structure of V-SBA-1 materials, which is in agreement with the results of XRD shown in Figures 1 and 2. The surface area, pore volume, and average pore diameter of V-SBA-1 were dependent on the synthesis conditions. For example, the samples B and D prepared at higher HCl content showed slightly lower values (surface area, pore volume, and pore diameter) compared to the samples A and C, respectively.

(19) Kruk, M.; Jaroniec, M.; Ryoo, R.; Kim, J. M. *Chem. Mater.* **1999**, *11*, 2568.

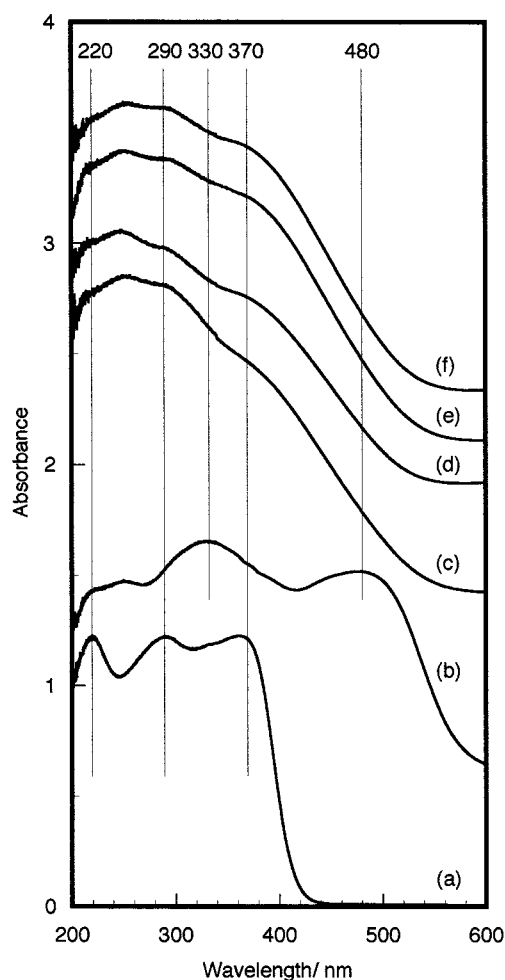


Figure 6. Diffuse reflectance UV-vis spectra of the various calcined samples and reference compounds: (a) NH_4VO_3 ; (b) V_2O_5 ; (c) V-SBA-1(A); (d) V-SBA-1(B); (e) V-SBA-1(C); (f) V-SBA-1(D).

Diffuse reflectance spectra in the UV-vis region of as-synthesized and calcined V-SBA-1 samples and those of reference compounds are shown in Figures 5 and 6. Considerably similar UV-vis spectra for the various V-SBA-1's were observed. In the UV-vis spectra of as-synthesized V-SBA-1 samples (Figure 5), absorption bands at about 220, 290, and 370 nm were observed. These absorption bands were closely matched with those of NH_4VO_3 as the reference compound. The band near 220 nm and those at 290 and 370 nm can be attributed to the charge transfer of tetrahedrally coordinated V^{4+} and V^{5+} ions,^{8,20-23} respectively, which suggested the incorporation of vanadium into the framework of SBA-1 materials. The bands at 290 and 370 nm can be assigned to tetrahedral V^{5+} ions at two different sites, that is, inside and outside the walls of the cubic SBA-1 structure.^{8,20}

After calcination in air, the color of V-SBA-1 samples changed from yellowish brown to white. When the

(20) Luan, Z.; Zhao, D.; He, H.; Klinowski, J.; Kevan, L. *Stud. Surf. Sci. Catal.* **1998**, *117*, 103.

(21) Chao, K. J.; Wu, C. N.; Chang, H. *J. Phys. Chem. B* **1997**, *101*, 6341.

(22) Kornatowski, J.; Wichterlova, B.; Jirkovsky, J.; Löffler, E.; Pilz, W. *J. Chem. Soc., Faraday Trans.* **1996**, *92*, 1067.

(23) Centi, G.; Perathoner, S.; Guelton, M. *J. Phys. Chem.* **1992**, *96*, 2617.

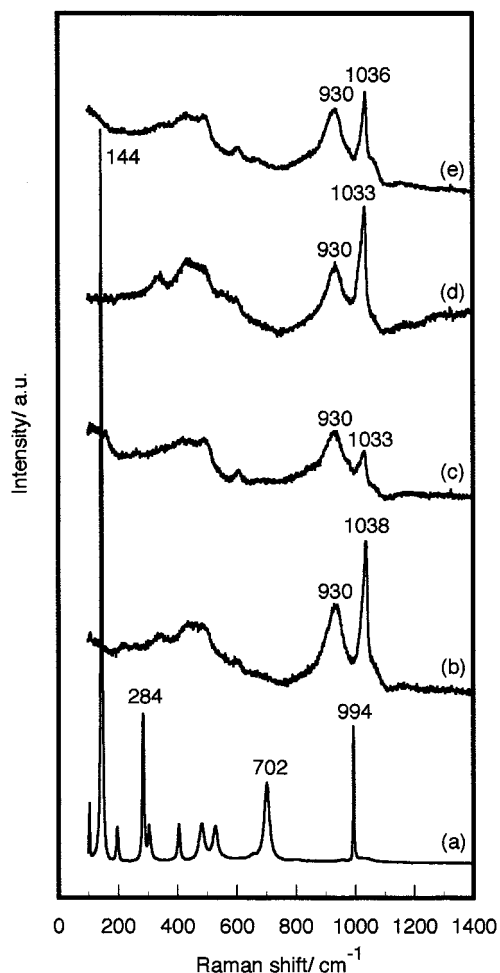


Figure 7. Laser Raman spectra of various calcined samples and reference compounds: (a) V_2O_5 ; (b) V-SBA-1(A); (c) V-SBA-1(B); (d) V-SBA-1(C); (e) V-SBA-1(D).

calcined V-SBA-1 samples were exposed to the ambient air, the color turned into bright yellow and then orange. This indicated that the additional coordination of water molecules to the V^{5+} ions as reflected by the broadening of the UV-vis spectra toward lower energy (>400 nm),^{8,9,21,22} as shown in Figure 6c-f. It is well-known that the charge transfer transition near 415 nm was generally observed for the yellow V^{5+} species with square pyramidal coordination, and the charge-transfer absorption at around 450 nm was related to the orange V^{5+} ions with distorted octahedral coordination.^{8,21-23} Similar to the as-synthesized samples (Figure 5), the calcined forms of the V-SBA-1 samples exhibited obvious bands at 290 and 370 nm (Figure 6), indicating the presence of tetrahedral V^{5+} species with V=O bonds. It should be noted that the absence of typical bands at ≈ 330 and 480 nm of reference V_2O_5 in the spectra of as-synthesized and calcined V-SBA-1 materials (Figures 5c-f and 6c-f) implies that no crystalline V_2O_5 was formed and the vanadium species was isolated and presented as a highly dispersed state in the framework of V-SBA-1 samples.

Figure 7 shows the laser Raman spectra of various calcined V-SBA-1 samples and reference compound of crystalline V_2O_5 . It is clear that no crystalline V_2O_5

phase was detected in the V-SBA-1 series products (Figure 7b-d) because there were no Raman bands at 994, 702, 284, and 144 cm^{-1} corresponding to the reference V_2O_5 .²⁴⁻²⁶ This also suggested that the vanadium species in V-SBA-1 was isolated and highly dispersed on the surface. The V-SBA-1 samples had a strong Raman band at around 1033–1038 cm^{-1} , which corresponded to the terminal V=O stretching vibration of the isolated tetrahedral VO_4 species.^{21,22,25} A broad band near 930 cm^{-1} could be assigned to a $V(OH)_2$ species formed by hydrolysis of the vanadyl V=O group located at the V ions in the center of a square pyramid.^{22,27} Because the V-SBA-1 samples were certainly hydrated in the ambient environment as mentioned above and the square pyramidal vanadyl complexes have been found in these samples (yellow color with corresponding UV-vis spectra of Figure 6c-f), the observed results from laser Raman spectroscopy were in agreement with those from UV-vis spectroscopy.

Noteworthy is that the intensity ratio of the 1033- cm^{-1} band to the 930- cm^{-1} mode in the spectra of V-SBA-1 samples (Figure 7b-e) was quite different. For the samples A and C synthesized at relatively low HCl content (HCl/ H_2O = 5/125 and 10/250), the Raman band near 1033 cm^{-1} (terminal V=O vibration) predominated in comparison with the band near 930 cm^{-1} ($V(OH)_2$ species), which formed from the hydrolysis of the V=O group in an ambient environment.^{22,27} In the case of samples B and D prepared at higher acidity (HCl/ H_2O = 10/125 and 20/250), the proportion of intensities of 930 cm^{-1} to those of 1033 cm^{-1} was considerably increased with increasing HCl content in the starting gel. Thus, it can be considered that the characteristics of isolated vanadium species in V-SBA-1 synthesized at different acidic conditions seem to be somewhat different.

Conclusion

A considerably large amount of vanadium (Si/V < 20) could be successfully incorporated into the SBA-1 mesophase at strongly acidic conditions. The obtained V-SBA-1 materials were characterized as possessing a highly ordered cubic structure (with two types of mesopores) and high surface areas (>1000 m^2 g^{-1}). The UV-vis and laser Raman investigations indicated that atomic vanadium oxides were present in a highly dispersed state and that the tetrahedrally coordinated vanadium oxide species was included in the SBA-1 mesophase.

Acknowledgment. We acknowledge financial support of New Energy and Industrial Technology Development Organization (NEDO). L.-X. Dai was supported by a fellowship from NEDO.

CM0005844

(24) Whittington, B. I.; Anderson, J. R. *J. Phys. Chem.* **1993**, *97*, 1032.

(25) Das, N.; Eckert, H.; Hu, H.; Wachs, I. E.; Walzer, J. F.; Feher, F. J. *J. Phys. Chem.* **1993**, *97*, 8240.

(26) Went, G. T.; Oyama, S. T.; Bell, A. T. *J. Phys. Chem.* **1990**, *94*, 4240.

(27) Schraml-Marth, M.; Wokaun, A.; Pohl, M.; Krauss, H.-L. *J. Chem. Soc., Faraday Trans.* **1991**, *87*, 2635.